Dehydration diffusion of $B(OH)_4$-sodalite investigated by micro-Raman spectroscopy on single crystals and combined TG/IR on powders

C. H. Rüscher[1]*, F. Kiesel[1], A. Wollbrink[2], L. Schomborg[1], J. C. Buhl[1]

[1]Institute for Mineralogy, Leibniz University of Hannover, Germany
[2]Institute for Physical Chemistry and Electrochemistry, Leibniz University of Hannover, Germany
*c.ruescher@mineralogie.uni-hannover.de

Abstract

Dehydration experiments were carried out on larger $B(OH)_4$-sodalite single crystals, $Na_8[Al_6Si_6O_{24}](B(OH)_4)_2$, at temperatures 300°C, 350°C and 400°C. Profiles of relative intensity variations of B-(OH)/Si-O vibration could be measured by micro-Raman spectroscopy ranging typically between 5 and 40 μm into the interior of the crystals. Profile analyses reveal effective dehydration diffusion coefficients D_{OH} between 10^{-11} and 10^{-9} cm^2/s with an Arrhenius activation energy $E_a \approx 1.3$ eV. H/D exchange experiments were realized at temperatures 50, 100 and 150°C in closed tubes. Profiles of OD/OH Raman intensities reveal effective H/D exchange diffusion coefficients D_{HD} between $1.5 \cdot 10^{-10}$ and $4 \cdot 10^{-11}$ cm^2/s with $E_a \approx 0.4$ eV. The dehydration effect for crystalline powders was reinvestigated up to 500°C in TG experiments and by IR spectra. These data show that dehydration takes place forming $NaBO(OH)_2$- and $NaBO_2$-sodalite centered at temperatures 250°C and 410°C, respectively. It is discussed that diffusion coefficients D_P could be estimated using the mass losses for the two stages of dehydration related to the experiments on the polycrystalline samples. Linear extrapolation of D_{OH}, i.e. the diffusion coefficients obtained on larger single crystals, towards lower temperature well approximates D_P using the dehydration effect obtained for crystalline powders between 140 and 180°C assuming spherical crystals of 0.1 μm diameters. H/D exchange could occur with proton/deuteron jumps through the four-ring windows of the sodalite framework. Larger ions or molecules predominantly pass through the six-ring windows which requires window opening.

Keywords: sodalites, dehydration diffusion, H/D exchange diffusion, micro-Raman spectroscopy

1. Introduction

Sodalites (SOD) form a group of compounds with interesting fundamental aspects in zeolite chemistry. An overview on the sodalite framework and on symmetry relationships of SOD type crystal structures has been given [1, 2]. SOD consists of closed packed truncated octahedral cages (toc-units) made in case of alumino-silicate framework from 24 $(Si/Al)O_4$ tetrahedral type units. These units form six-rings and four-rings in common with neighboring cages. The capability of the sodalite structure for incorporating various cations and anions of different sizes can be explained by the large flexibility through the tilt mechanism and the tetragonal distortion of the AlO_4 and SiO_4 tetrahedra as shown in the perspective view in Fig. 1 (after [3]). Generally the alumino-silicate sodalite framework requires three positive charges per cage, e.g. Na-cations, for charge compensation, i.e. 6 Na^+ per unit formula. As for example in the mineral sodalite with the ideal formula $Na_8[Al_6Si_6O_{24}]Cl_2$ there are two additional Na^+ introduced together with the two Cl-anions. Whereas the Cl^- occupy special position in the center of each cage, at (0,0,0) and (0.5,0.5,0.5) the 8 Na^+ become structurally indistinguishable on the 8e (xxx) position in space group P-43n close to the six-ring windows.

There are many publications on sodalites who used the ion exchange effects, e.g. for the investigation of structural effects in the solid solution type systems $Na_{1-x}M_x$-SOD, M = Rb, K, Li, with appropriate solutions or melts [4, 5] or as shown more recently using polyethylene oxide solvents [6]. However, studies on the quantification of ionic diffusion in sodalites seem surprisingly rare. It has been noticed at the very early stage in zeolite chemistry that ion exchange effect and ion sieve action occur in sodalites as solid state reaction closely dependent upon diffusion [7].

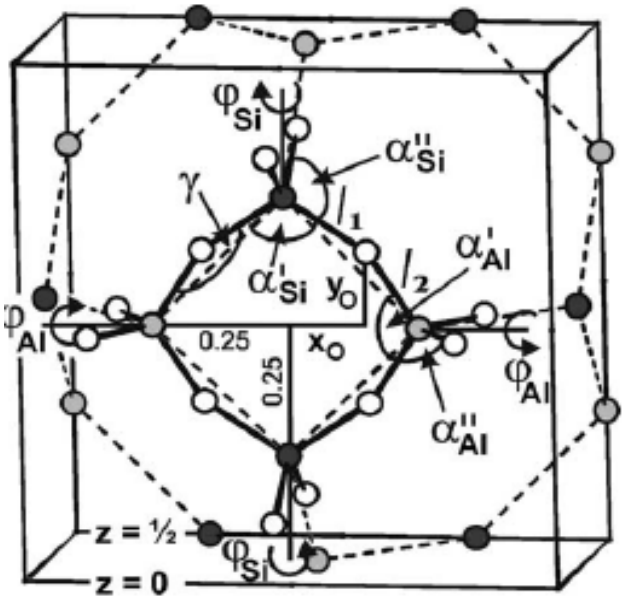

Figure 1: Perspective view of one half of the sodalite cage depicting six-ring and four-ring windows (dashed lines) (after [3]). Filled black and grey circles denote Si and Al positions. Open circles show oxygen of TO_4-units for the four-ring in the 100 plane. Tilt angles (φ), tetragonal tetrahedral distortions (α', α''), Si-O-Al angle and bonding length (l1, l2) are depicted as denoted.

In such studies so called basic sodalites were investigated. Basic sodalites are sodalites with an OH^- anion instead of Cl^-, and include additional water molecule in the cages. Hydroxy sodalite, also called basic-hydosodalite, $Na_8[Al_6Si_6O_{24}](OH)_2{\cdot}2H_2O$, and hydrosodalite $Na_6[Al_6Si_6O_{24}](H_2O)_8$ could be seen as the end members of hydro-hydroxy sodalites [8, 9] where cage opening effect occur with increasing the hydro component due to a reduction in Na occupation. Investigation of dielectric properties of such sodalites under hydrated and anhydrous conditions, indicate that the leading current carriers could be protons and probably Na^+/OH^-, respectively [10]. A high proton transfer between OH^- and "zeolitic water" H_2O could be assumed estimating diffusion coefficients $D = 1.7{\cdot}10^{-11}$ and $2.3{\cdot}10^{-11}$ cm^2/s at 30°C and 50°C, respectively. No estimates on Na^+ or OH^- diffusion could be provided, however. In this respect Sippel [11] could provide Na tracer diffusion data for temperatures 476°C ($2{\cdot}10^{-11}$ cm^2/s), 546°C ($1.1{\cdot}10^{-10}$ cm^2/s) and 623°C ($5{\cdot}10^{-10}$ cm^2/s) using a radio autography technique on sectioning of crystal pieces of the mineral sodalite. These first Na-self diffusion data could probably be improved by Levi and Lutze [12] who used at that time a most straight forward method of isotopic exchange on single crystal spheres in molten salts ($NaNO_3$, NaCl) for temperatures between 450 and 850°C. A more recent diffusion related study on sodalites has been reported on the exchange of anions like F, Br and J in NaCl-SOD, too. A significant Br/Cl exchange was obtained in the micrometer rim of crystals at temperatures between 800 and 1000°C which could have implications for interpretations of fluid compositions during rock formation [13].

Here we may report our new results on the dehydration of $NaB(OH)_4$-SOD: ideally $Na_8(Al_6Si_6O_{24})(B(OH)_4)_2$. Crystallization kinetics and crystal structure analysis of $NaB(OH)_4$-SOD has been reported [14, 15]. The stepwise dehydration of $B(OH)_4$-SOD [16] and formation of unusually coordinated boron BO_2- and $BO(OH)_2$-anion species has been described [17]. The stepwise formation of these species and the instability of $NaBO_2$-SOD during heating above 500°C were also obtained in temperature dependent infrared absorption experiments [18]. The mechanism of dehydration of $NaB(OH)_4$-sodalite could also be of some renewed interest. $NaB(OH)_4$-SOD appears as the endmember of the hydrogen release reaction of $Na_8(Al_6Si_6O_{24})(BH_4)_2$ ($NaBH_4$-SOD) [19, 20]. In further reaction steps species of the type $BO(OH)_2^-$ and BO_2^- in the sodalite cages were also obtained. These species could also be rehydrated. The water content could then be used for the further hydrogen release [21].

The measurement techniques of mass transport in zeolites are nowadays highly advanced. There exist a number of review papers, e.g. on macroscopic methods for measuring micro-pore diffusion [22], in-situ characterization techniques [23], and microscopic diffusion measurement technique [24]. Herein surveys of techniques are given including pulsed field gradient NMR (PFG NMR), quasi

elastic neutron scattering (QENS), or interference microscopy (IFM) and IR microscopy (IRM) besides other sorption/desorption rate measurements including monitoring pressure variation or chromatographic methods. In so far the application of micro-Raman spectroscopy as shown here to be useful for the detection of profiles on micro-meter scale resolution could also be new in the field.

2. Experimental

Clear tetrahydroxoborate sodalite single crystals of sizes typically up to 0.5 mm in diameter were synthesized earlier as described in detail by Buhl et al. [14] hydrothermally in steel autoclaves with an interior volume of 8 ml. Silver tubes with a diameter of 6 mm and 80 mm length were used as sample containers. For starting substances sintered kaolinite (Fluka 60609), 2 h at 1500°C, boric acid (Riedel-de Haen 31146) and 8 M NaOH solution (Riedel-de Haen 30620) were used. In the hydrothermal solution a starting B_2O_3/Al_2O_3 ratio of 10.0 was set by using a boric acid concentration of 5.4 M. The experiments were carried out in the temperature range of 200 – 500°C at pressures of 100 – 150 MPa. After a reaction period of 5 days the product were repeatedly washed with water. Also, tetrahydroxoborate sodalite powders were produced hydrothermally in steel autoclaves with an interior volume of 50 ml. For synthesis 1 g kaolinite (Sigma-Aldrich K7375), 4 g boric acid (Merck) and 12.5 ml 8 M NaOH solution (Merck) were used. The experiments were carried out at a temperature of 200°C. After an experiment time of 2 days the product were repeatedly washed until a pH of 9 was obtained. According to X-ray analysis this produced a single phase $NaB(OH)_4$-SOD polycrystalline material.

Single crystals were dehydrated at ambient pressure and temperatures of 300, 350 and 400°C with dwell times between 0.5 and 24 h under controlled conditions using a *Setaram Setsys Evolution 1600* thermo analyzer and 5 ml corundum crucibles. The heating and cooling rate were set to 5 K/min. Technical air (80 % N_2, 20 % O_2) with an gas flow of 20 ml per minute was used as carrier gas. For H/D exchange experiments selected single crystals were put into Teflon cups using 6 ml of 90 % D_2O/10 % H_2O liquid (Merck). The closed Teflon cups were heated in series for 24 h at 50°C, 10 h at 100°C and 4 h at 150°C. Cooling and heating were within 0.5 h. Powder samples were dehydrated at temperatures between 80 and 500°C with a dwell time of 10 min using the same thermo analyzer with 5 ml corundum crucibles. The heating and cooling rate were set to 5 K/min and helium with a gas flow of 20 ml per minute was used as carrier gas.

Depth profiles (steps between 1 and 5 µm) of selected single crystals after heat treatment as well as after H/D exchange experiments were measured in crack free crystal areas by Raman spectroscopy. The measurements were made on a confocal *Bruker Senterra* micro-Raman spectrometer equipped with an Olympus BX 51 microscope and an Andor DU420-OE CCD camera. Depolarized spectra were collected at ambient conditions, using the 532 nm laser excitation lime with 20 mW power, under 50 x magnification of an Olympus LWD objective for 1 s with 10 times acquisition repetitions. Instrumental precision was within ± 3 cm^{-1}. Fourier transformation infrared spectroscopy analyses of the powder samples before and after heat treatment were performed on a *Bruker Vertex 80v* FTIR spectrometer. The measurements were carried out in the mid-IR range from 370 to 5000 cm^{-1} with a resolution of 2 cm^{-1}. The sample preparation was conducted by the KBr pellet method, with 0.65 mg of sample diluted in 199 mg of KBr. Some IR transmission spectra were taken on thin slices of the single crystals using an attached IR-microscope (*Bruker IFS88/IR scopeII*).

3. Results

3.1 Single crystal experiments

Examples of crystals as they appear before and after the dehydration experiments and the heat treatment in D_2O are shown in Fig. 2. No visible changes of the single crystals were observed for short time heat treated in D_2O, whereas after longer experiments the crystals became opaque/milky. Those crystals were not investigated further. Crystals heated to 300, 350, 400°C generally gain cracks as observed in Fig. 2. These crystals were further investigated in crack free parts using the micro-Raman technique.

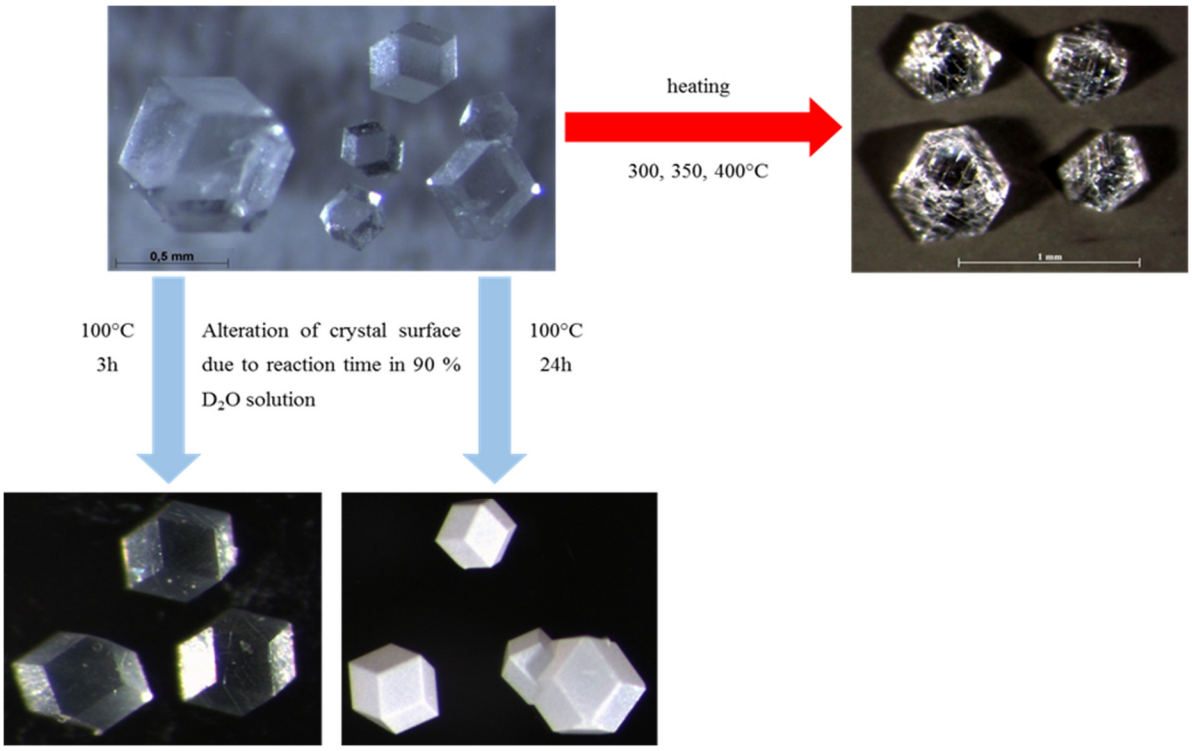

Figure 2: Photographs of selected crystals before and after different alterations as described.

Typical spectra obtained in depth profiles for an example of crystal dehydrated for 0.5 h at 400°C are shown in Fig. 3 in the range between 400 and 1100 cm^{-1}. Beside the strongest $NaB(OH)_4$-SOD specific lattice vibration (symmetric Si-O) at about 444 cm^{-1} ($\nu_{Si\text{-}O}$) and its B-$(OH)_4$ vibration at 849 cm^{-1} ($\nu_{B\text{-}OH}$) some weaker peaks appear between 1000 and 1050 cm^{-1} assigned to asymmetric Si-O vibrations. A peak at about 861 cm^{-1} appears when measured at the crystal surface looses gradually in intensity with increasing steps into the crystal. This peak is an indication of cage filling species of $BO(OH)_2$-anions obtained from the loss of effectively one molecule H_2O.

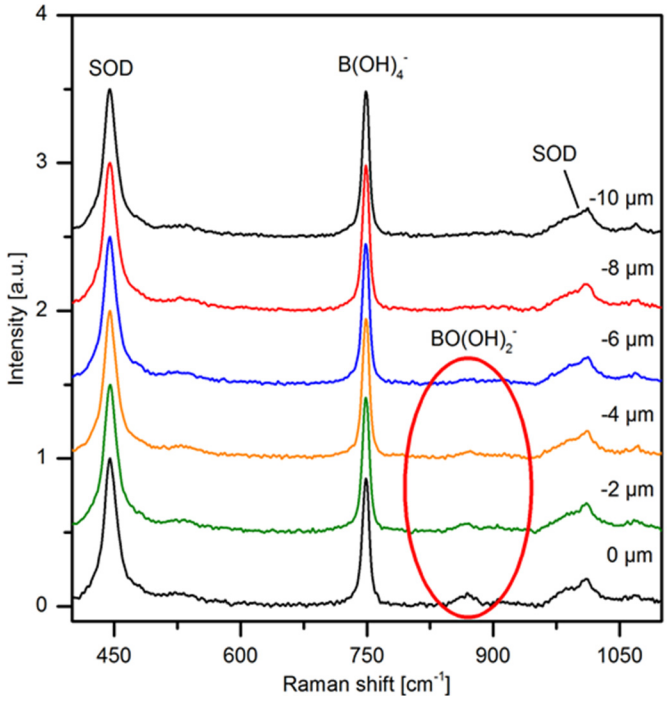

Figure 3: Raman spectra along a depth profile showing vibrations of $[BO(OH)_2]$-species beside $[B(OH)_4]$ cage fillings and characteristic SOD-framework peaks for a crystal heated 0.5 h at 400°C.

The spectra were evaluated using the relative change in intensity $n_x = (v_{B\text{-}OH}/v_{Si\text{-}O})/f$ obtained at different depth normalized to $f = v_{B\text{-}OH}/v_{Si\text{-}O}$ in the depth when f becomes constant. Examples of depth profiles and rechecked in cross sections are shown in Fig 4. It is interesting to note that cracks behave to more or less extend as a surface, i.e. observing the same type of profile. Thus it was checked that no active cracks could obscure the values. In a first step the profiles were used for an estimate along

$$D_1 = z^2/t \tag{1}$$

With t = holding time and z taken as the depth at half the relative intensity at surface n_s (compare dashed lines in Fig. 4). A further evaluation were carried out along

$$x = erf(0.5 \cdot x \cdot (D_2 t)^{-0.5}) \tag{2}$$

where n_x values were normalized as $x = (n_x\text{-}n_s)/(n_0\text{-}n_s)$, n_s and n_0 being the relative intensities at the surface and the not dehydrated one, respectively. Eq. 2 holds for semi-infinite media as given by Crank [24]. Table 1 lists the obtained diffusion coefficients D_1 and D_2.

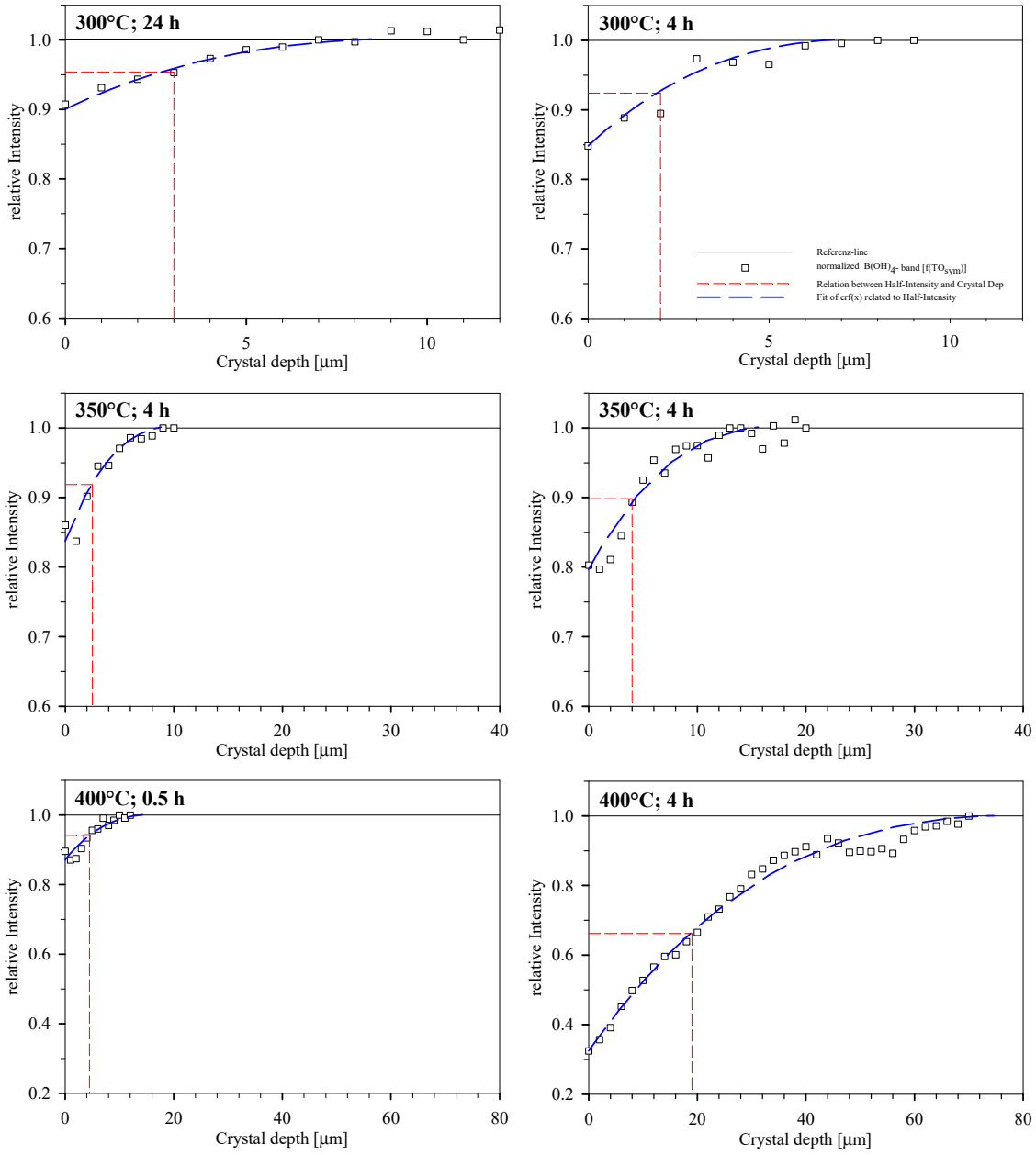

Figure 4: Selected examples obtained in depth profiles (left side) and cross section (right side) at temperatures as denoted. Dashed vertical and horizontal lines denote first step of evaluation and dashed blue line along with eq. 1 and 2, respectively (compare text).

Raman spectra in the area of 800 to 3800 cm^{-1} obtained along a typical depth profile for a single crystal bathed in D_2O at 50°C for 24 h are shown in Fig. 5a. The OD related Raman vibration band at 2691 cm^{-1} decreases in intensities with depth while the OH related Raman band at 3640 cm^{-1} increase. The relative change in intensity is shown in Fig. 5b. The profiles of relative change of OD/OH were evaluated. Effective diffusion coefficients are given in Tab. 1.

A clear distinction between $NaB(OH)_4$-SOD, $NaBO(OH)_2$-SOD and $NaBO_2$-SOD could be achieved in Raman spectra, too (not shown). For the fully dehydrated phase the O-H (at 3600 cm^{-1}) and B-(OH) (at 841 cm^{-1}) peaks are absent, as well as the $BO(OH)_2$ related peak at 861 cm^{-1}. The effect of dehydration as measured by micro-Raman technique on large and crack free areas of crystals reveal only the first step of dehydration with the appearance of $BO(OH)_2$ cage fillings at temperatures 300, 350 and 400°C. Thin slices of some crystals in transmission mode were investigated using micro-IR, too. The spectra reveal some indication of bending and stretching vibrations assigned to H_2O molecules beside the main peak at 3640 cm^{-1} of the $[B(OH)_4^-]$ species, which could, however, not be detected in its whole strength even for the thinnest plate available (30 µm thick) due to its high intensity. An evaluation of the intensity of the H_2O contribution suggests a content of about 1.4 wt%.

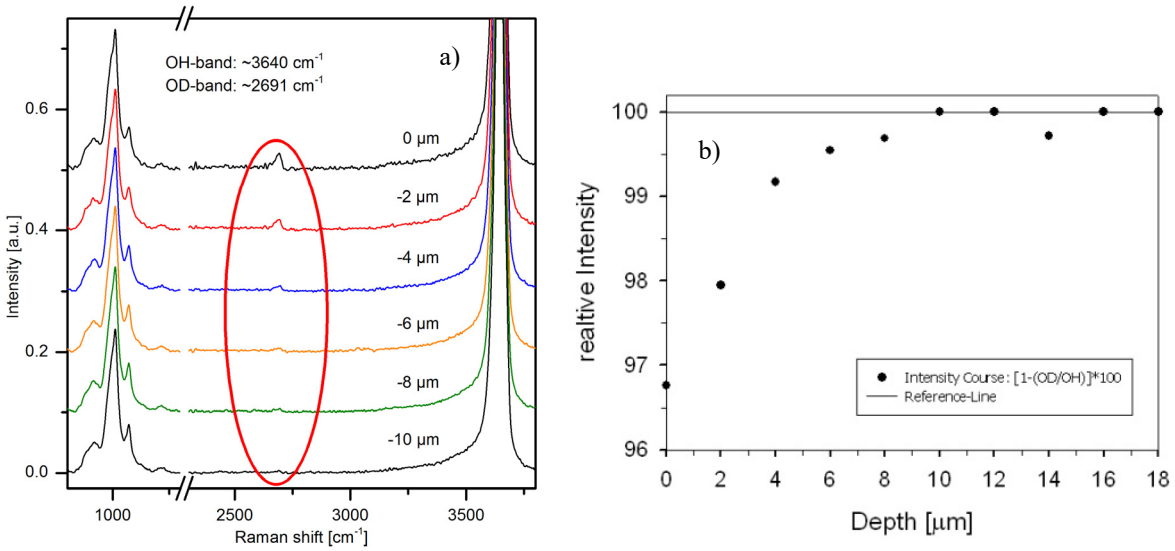

Figure 5: a) Spectra obtained for a crystal in depth profiling focused on OD intensity at the surface and its gradual decrease focusing in steps into the crystal. b) The relative change of OD/OH related peak intensity from the surface into the interior of a crystal.

Table 1: Diffusion coefficients D_1, D_2, obtained with eq. 1 and 2 as described in the text and D_{HD} from exchange experiments as described in the text.

Temperature [°C]	log D_{OH1} [cm²/s]	log D_{OH2} [cm²/s]
300	-11.81	-11.33
300	-11.81	-11.24
300	-11.84	-11.08
300	-11.84	-
350	-10.95	-10.38
350	-10.95	-10.46
350	-10.53	-10.46
350	-10.68	-10.23
400	-10.35	-9.45
400	-10.16	-9.47
400	-10.17	-9.56
400	-10.05	-

Temperature [°C]	log D_{HD} [cm²/s]
50	-11.98
50	-11.54
50	-11.73
50	-11.38
50	-11.63
100	-10.95
100	-11.08
100	-11.05
100	-10.92
150	-10.16
150	-10.35
-	-

3.2 Powder related experiments

The first step of dehydration investigated here in the micro-Raman spectra is seen at significant lower temperatures on polycrystalline materials as reported in the literature [18]. Therefore, similar experiments were carried out here in combined TG/DTA and IR experiments. IR spectra obtained for the starting sample and samples obtained after the TG heating experiments are shown in Fig. 6. The IR spectra of the starting material show the typical vibration bands of the sodalite framework in the lower wavenumber range of 400 – 1100 cm^{-1} as well as the OH related vibration band of the $[B(OH)_4]$ cage fillings at 3640 cm^{-1}. At 140°C the absorption peaks indicative for $[BO(OH)_2^-]$ species occur at 1230, 1475 and 3592 cm^{-1}. With increasing temperature the intensities of these bands increase while the intensity of the $[B(OH)_4^-]$ species decreases. At 275°C first indications of the $[BO_2^-]$ species could be seen with the appearance of absorption peaks at 1955 (^{11}B-O_2) and 2030 cm^{-1} (^{10}B-O_2). Between 275 and 350°C $[BO_2^-]$-, $[BO(OH)_2^-]$- and $[B(OH)_4^-]$-cage filling species were observed together. Above 350°C the OH absorption peak of the $[B(OH)_4^-]$ cage filling species could not be detected in the IR spectra anymore and above 450°C only $[BO_2^-]$ species could be seen. The results are tentatively in agreement with earlier data obtained in in-situ temperature dependent infrared (TIR) absorption spectra [18] in so far as the same sequence had been described earlier, however shifted by about 100°C towards higher temperature. This could probably be explained by larger crystals sizes of the polycrystalline samples used earlier (see discussion below).

Table 2: Relative mass loss, volume fraction (f) and trial diffusion coefficients (D_p) using eq. 5 along with eq. 1 with r_1 = 0.075 µm, r_2 = 0.05 µm for the polycrystalline powders in the TG experiments.

Temperature [°C]	Relative mass loss [%]	Volume fraction [%]	log D_P r_1 [cm²/s]	log D_P r_2 [cm²/s]
140	0.78	8.21	-16.14	-16.47
150	0.94	13.04	-15.73	-16.05
160	1.16	19.29	-15.37	-15.69
170	1.47	28.49	-14.99	-15.32
180	1.60	32.21	-14.87	-15.20
190	1.63	33.18	-14.84	-15.16
200	2.06	45.87	-14.51	-14.83
210	2.37	54.75	-14.31	-14.64
220	2.47	57.86	-14.25	-14.57
250	2.94	71.57	-14.23	-14.56
275	3.60	-	-	-
350	4.89	28.69	-14.99	-15.31
400	6.05	62.61	-14.11	-14.48
450	6.82	85.14	-13.70	-14.02
500	6.88	86.93	-	-

Examples of TG curves obtained during heating to 80, 120, 250, 350 and 500°C, during holding at that temperature and their cooling curves are shown in Fig. 7. For each TG run carried out the obtained mass losses are collected in Tab. 2. Further data given in Tab. 2 are discussed below. For the 500°C run the differentiated dTG curve is shown in addition to the TG curve. Two main peaks with minima at around 250 and 420°C are observed in the dTG curve. The dTG curve well coincides with DTA curves, showing the same peak distribution as endothermic signals. The minima are related to the two main dehydration steps, respectively:

$$[B(OH)_4]_{SOD} => [BO(OH)_2]_{SOD} + H_2O \quad (3)$$

$$[BO(OH)_2]_{SOD} => [BO_2]_{SOD} + H_2O \quad (4)$$

A shoulder at about 100°C indicates further dehydration effect from some additional weakly bound H_2O. This contribution could be estimated to account not for more than 0.5 wt% of the total loss. According to this a total mass loss of about 6.3 wt% is related to the dehydration steps eq. 2 and 3.

Ideally $NaB(OH)_4$-SOD could lose 6.8 wt% related to eq. 1 and 2. The lower value observed experimentally indicate therefore the presence of some impurity phase which could well be related to X-ray amorphous contribution as detected in careful carried out XRD-pattern as a broad bump between 20° and 40° 2Theta. The additional water obtained in the TG-curves at temperatures up to 120°C could well be related to be adsorbed herein. Indications of additional water could also be detected in the IR-spectra showing weak additional absorptions at about 1630 cm^{-1} and between 3000 and 3600 cm^{-1}.

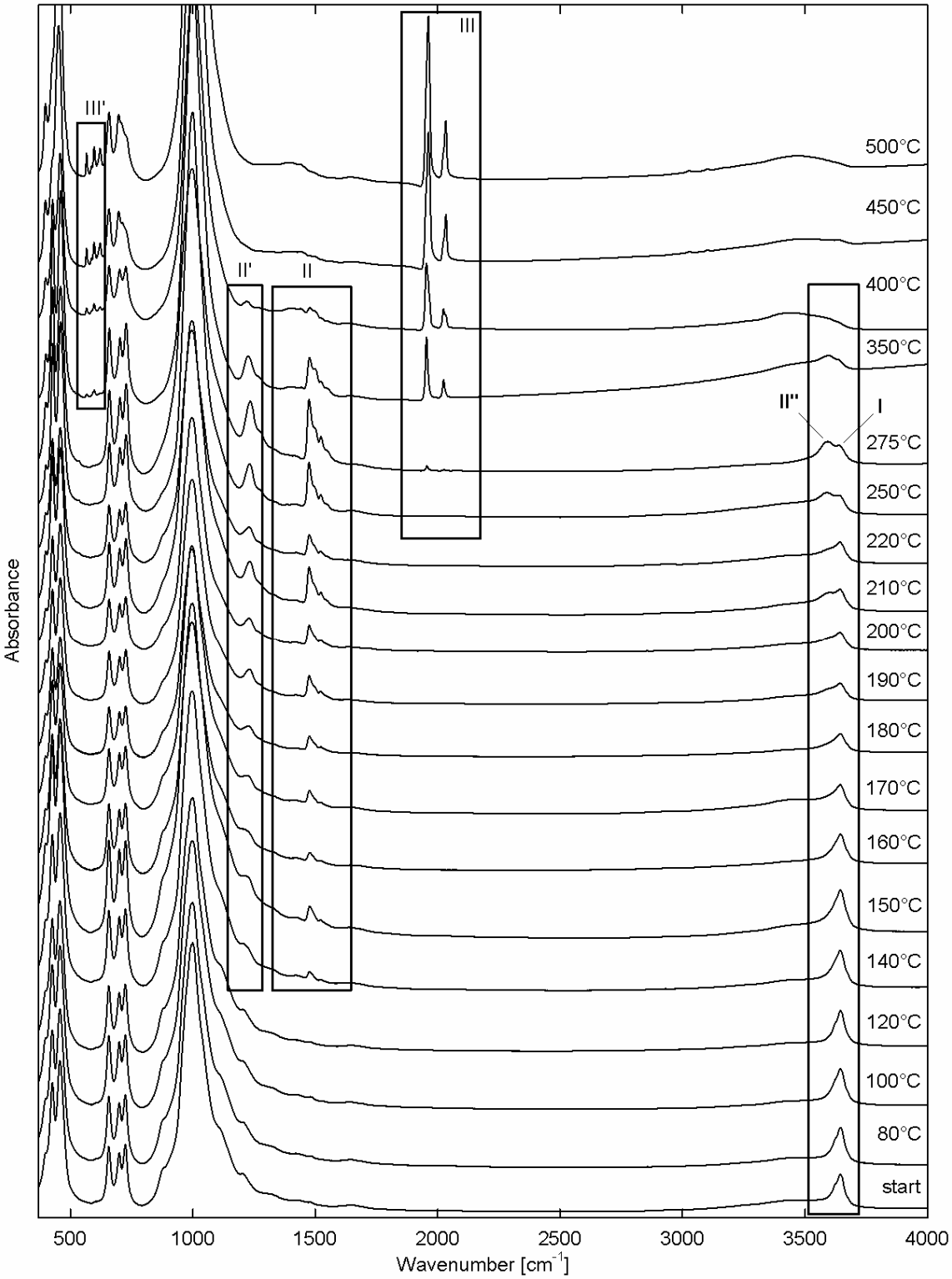

Figure 6: IR spectrum of the starting sample and spectra given after TG measurements with holding temperatures as denoted. Characteristically peaks for $B(OH)_4$- (I), $BO(OH)_2$- (II, II', II'') and BO_2- (III, III') species are marked (compare text).

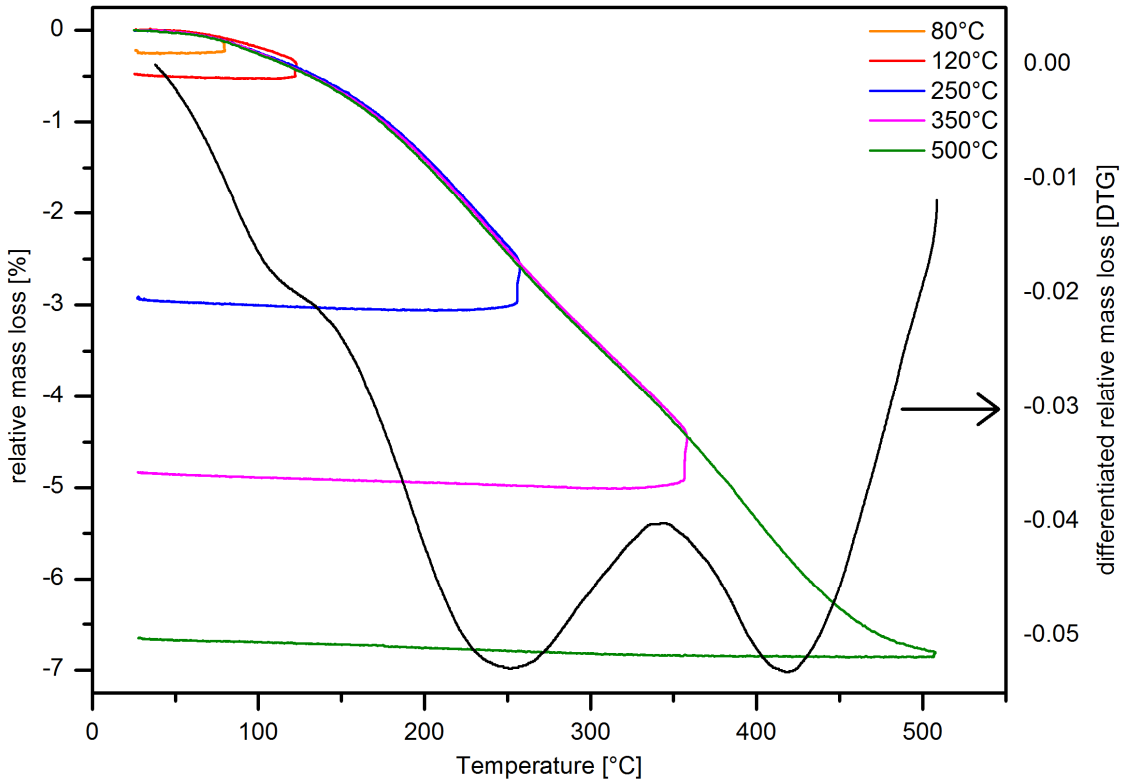

Figure 7: TG curves for heating and cooling runs to holding temperatures as denoted. For the 500°C the diffentiated dTG curve for the heating run is also shown.

4. **Discussion**

Arrhenius plots of the dehydration diffusion coefficients D_{OH} (D_1, D_2) and the exchange coefficients D_{HD} obtained using the micro-Raman technique are shown in Fig. 8. Also shown are data of Na-self diffusion and Cl/Br exchange data reported earlier as denoted in the introduction. Additional data shown are some estimated dehydration diffusion coefficients D_P using the powder related mass losses from the TG data (Tab. 2) which will be further discussed below.

A linear regression to D_{HD} in the Arrhenius plot reveals activation energy of $E_{HD} \approx 0.44$ eV. Linear regressions to D_1 and D_2 in the Arrhenius plot are shown as dashed line. They are largely parallel providing an activation energy of about $E_{OH} \approx 1.3$ eV for $\log(D_{OH})$. The obvious factor between D_1 and D_2 is $2\sqrt{\pi}$. This can be seen as a correction to eq. 1 taking into account the total amount of diffusing species which left the semi infinite medium according to Crank [24]. The diffusion coefficients are related to the number of dehydrated cages forming $BO(OH)_2$-species relative to $B(OH)_4$-ones and the exchanged B(O-D) relative to B(O-H)-groups for D_{OH} and D_{HD}, respectively. Since the diffusion coefficients are in the same order of magnitude the obtained profiles look quite similar, spreading to the same depth and intensity observable by the micro-Raman technique. However, the effect of HD-exchange is obtained in a range of much lower temperature, 50-150°C, compared to the first step of dehydration (eq. 3), 300-400°C. The extrapolation of D_{OH} towards lower temperatures indicates much smaller D_{OH} compared to D_{HD}. According to this, the dehydrated volume becomes less and less relative to the HD exchanged part compared at the same temperature. This indicates that the dehydration mechanism and the ability of proton mobility in $B(OH)_4$-SOD become more separated with decreasing temperature. For the HD exchange a defect formation in the proton sublattice of the $B(OH)_4$ cage filling species together with a proton jump through the four-ring windows (see Fig. 1) could be suggested. It seems to be unlikely that D_2O or H_2O or even OH-anions easily penetrate through the four-ring windows. The six-ring windows remain mostly closed by the Na-ions at the lower temperature. Thus for the dehydration mechanism it needs to be analyzed whether an opening of the six-ring window could be involved and how. In this respect the data reported by Levi and Lutze [12] for Na self-diffusion D_{Na} for NaCl-SOD could be meaningful. The framework of $NaB(OH)_4$-SOD appear to be more expanded, e.g. 9.02 Å compared to 8.88 Å at 20°C. This could probably imply a higher D_{Na} for $NaB(OH)_4$-SOD compared to D_{Na} in NaCl-SOD. It may be suggested that the

probability of formation of $BO(OH)_2$-cage filling species could not be higher than the ability of formation of Na vacancies, if not enhanced by other supporting effects.

The ability of defect formation in the Na-sublattice seems to be rather unlikely in "ideal sodalite" following some recent calculations. Schneider et al. [26] showed that ideal NaCl-SOD and $NaBH_4$-SOD shows a high stability against any significant distribution of Na-ions through the six-ring windows or rotation of the Na-tetrahedron within the cage. In this respect the data reported by Sippel [11] might be remarkable. These data show Na self diffusion coefficients at higher temperatures and higher activation energy, suggesting that any opening of the six-rings by intrinsic defect formation on Na sites could be negligible.

The answer to the question remains open whether the data of Sippel [11] or Levi and Lutze [12] could describe a Na-self diffusion behavior of NaCl-SOD more closely, either for a more or less ideal sodalite. On the other hand investigating the real crystal structure showed a significant ability for jumps of the Na-ion through the six-ring windows. A nearly equal distribution of Na-ions on sites above and below the six-ring windows is obtained in single crystal XRD structure analysis at about 450°C in $NaNO_3$-SOD [3]. Neutron diffraction studies have shown ionic diffusion path along [111] for Na-cations and even Cl-anions in NaCl-SOD which become more probable with increasing temperature [27]. These effects are related to thermal expansion of the sodalite and the libration motion of the $[TO_4]$-polyhedra leading to the untwisting of the framework (tilt angle reduction). Therefore, the exchange of Cl-anions by Br-anions as observed by Pan and Dong [13] in the outer micrometer thick rim of NaCl-sodalite crystals could indicate a diffusion controlled process at heating temperatures of 800 and 1000°C for some days [Fig. 8].

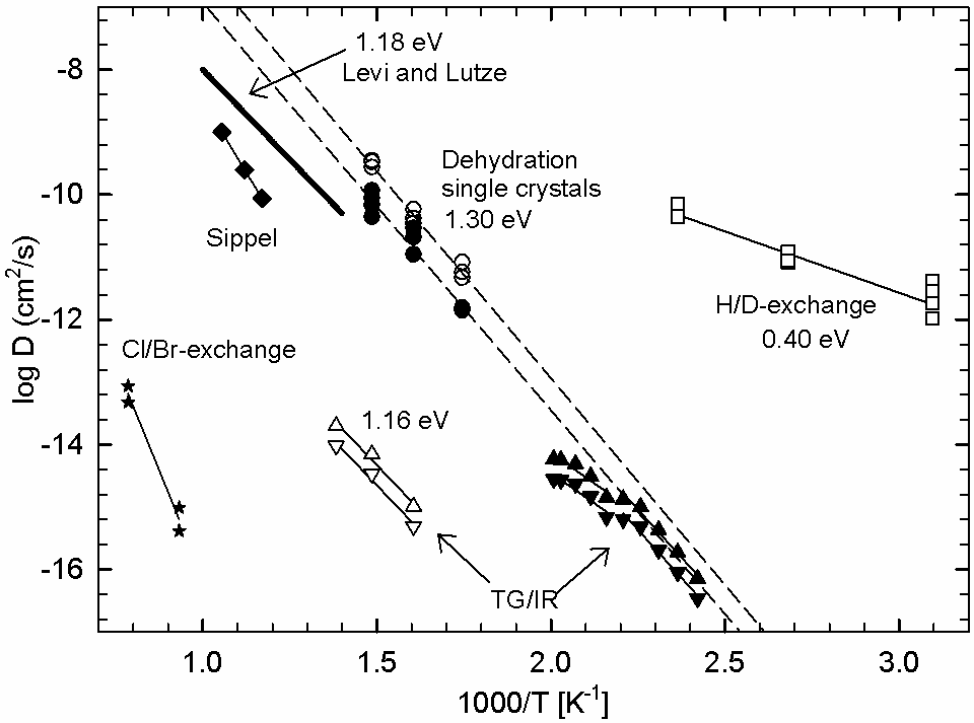

Figure 8: Arrhenius plot of dehydration diffusion coefficients D_1 (filled circles), D_2 (open circles) and H/D exchange diffusion coefficients (open squares) from micro-Raman profiles on single crystals. Dashed and solid lines are obtained from linear regression to respective data (filled (D1) and open circles (D2)) with linear regression lines (dashed). Filled and open triangles are trial diffusion coefficients calculated using the mass losses of polycrystalline powders as discussed in the text. Na-self diffusion data of NaCL-SOD as reported by Levi and Lutze [12] and Sippel [11] as well as diffusion data obtained in Br/Cl exchange experiments [13] of NaCl-sodalite are also shown.

In fact single crystal X-ray structure refinements of $NaB(OH)_4$-SOD implied a rather strong deviation of the chemical composition, $Na_{7.5}[Al_6Si_6O_{24}]B(OH)_4)_{1.5}\cdot 2H_2O$ [15]. The deficiency on Na (8e) positions were randomly occupied with $[Na_3(H_2O)^{3+}]$-cage fillings. With other words, 1 out of 4 cages could be a hydro sodalite, expecting 3.42 wt% H_2O. This seems to be an overestimate of the H_2O content of the presently used crystals where an estimate of the upper limit was 1.4 wt% according

to the H_2O related absorption intensity in the IR spectra. According to this only about 10 % of the cages could be hydro sodalite giving an average composition $Na_{7.9}[Al_6Si_6O_{24}]B(OH)_4)_{1.9}\cdot 0.8H_2O$. Nevertheless the single crystal refinements showed strong deviations in Na-oocupancies and require even a distribution over 4 split positions along [111]. Even Boron becomes slightly off-centered and could only be refined using a rigid $B(OH)_4$-body distributed randomly over 24i positions. It is interesting to note that some recent ab initio calculation also reveal a slight off centering of boron [28]. In that study the proton could be localized with O-H distances of 0.89 Å, too. Additionally, the $B(OH)_4$-body deviates significantly from being a tetrahedral. Thus there is a symmetry breaking of the sodalite structure and the cubic symmetry is only prevailed in average. This has been noted experimentally, too. E.g. it has been described that with increasing temperature, above about 90°C the peak splitting of the B(O-H) signal in the IR spectra disappear and there is an anomaly in the wavenumber shift in the three lattice modes v_1, v_2, v_3 related to a structural phase transition indicating a higher dynamic of the cage filling ions [18]. This implies that even without the assumption of a high number of $[Na_3(H_2O)^{3+}]$-cage fillings there could be a high tendency of formation of vacancies by intercage jumps or distortions from ideal positions giving a significant ability of ions or molecules to jump through the cage windows. This suggestion is supported by observations that rehydration of BO_2-SOD could be reached at room temperature conditions.

It seems intuitively plausible that diffusion through the sodalite cages could be enhanced for an occupation deficiency on Na-sites. An opening of the six-ring windows is given for hydrosodalite, $Na_6[Al_6Si_6O_{24}](H_2O)_8$, possessing practically a pathway through the sodalite cages. Hydrosodalite can be dehydrated starting at about 80°C, which is completed at temperatures between 230°C and 300°C [8, 9]. It has been described that an intermediate, $Na_6[Al_6Si_6O_{24}](H_2O)_4$, could be stabilized regarding to the two steps of dehydration centered around 130 and 230°C. Structurally the water molecules were located on the equivalent 8e positions opposite to the Na-ions in hydrosodalite, i.e. the six-ring windows become more and more opened with increasing degree of dehydration. It has been reported that the distribution of water in basic hydro-sodalite, $Na_8[Al_6Si_6O_{24}](OH)_2(H_2O)_4$ differ significantly, possessing three OH-groups per cage on opposite sides to the Na close to the six-rings. One of the two additional protons was localized in the center. The fifth proton of the cage filling complex $[Na_4H_2(OH)_3]^{3+}$ could not be localized [8, 9]. The first stage of dehydration loosing 1 H_2O per cage is centered at about 130°C, i.e. the same temperature as the first stage of dehydration for hydro sodalite, too. However, the mechanism of dehydration should be rather different and related to a strong influence of interaction with the framework and within the complex of cage filling species. Therefore it is interesting to note that there is only a smooth lattice expansion for basic hydro-sodalite, from about 8.91 to 8.92 Å for heating from 20 to 250°C. In the temperature range between 250 and 430°C the lattice parameter decreases to about 8.80 Å. This is the temperature range were another lost of 1 H_2O is observed, centered at about 380°C. For hydro sodalite both steps of dehydration are related with significant lattice expansion, from 8.85 Å (20°C) to 8.90 Å (120-130°C), to 8.95 Å (at 180°C), followed by a more steep increase to 9.08 Å (230°C).

In some respect $NaB(OH)_4$-SOD behaves similar to hydro-sodalite during dehydration, showing an increase in lattice parameter, first a slight increase between 9.00 Å (20°C) to 9.04 Å (250°C) followed by an increase to about 9.12 Å at about 500°C [16]. The two ranges cover clearly the formation of two phases, $NaBO(OH)_2$-SOD and $NaBO_2$-SOD, as depicted in the TG experiments and shown in the IR spectra of microcrystalline powders. The question arises how this phase formations could affect the postulated diffusion related mechanism of dehydration for $NaB(OH)_4$-SOD. An “ordinary diffusion” related mechanism of dehydration might be assumed in the limit of defect formation of some percentages of cage fillings of $BO(OH)_2$-species. For large single crystals this effect remains even below 5-10 % in a range covering few micro-meter even at temperatures well in the stability field of $NaBO_2$-SOD. The reason for this is that enough water is still supplied from deeper insight the crystal. It could be supplied either as molecule H_2O or separately as protons and hydroxyl groups. Since protons jump rather fast, as is indicated by the HD exchange experiments, a transport in form of ions could be favored. A conclusion about this needs, however, further investigations. Irrespectively of this we may try to use the single crystal data for an interpretation of the dehydration effects achieved at lower temperatures obtained on the polycrystalline material. For this purpose we may use the mass loss data tentatively. An estimate of a diffusion coefficient could be achieved assuming a crystal sphere of radius r and an exchanged volume fraction f considered as an outer shell of thickness z,

$$z = r(1-(1-f)^{1/3}) \tag{5}$$

which could be used as the penetration depth of diffusion front along with the diffusion time t at a constant temperature using eq. 1.

Ideally there can be a mass loss of 6.6 wt% if there is 100 % $NaB(OH)_4$-SOD converted to $NaBO_2$-SOD. The additional water obtained in the TG at temperatures up to 120°C has been subtracted in all cases. There is an obvious superimposition of the 1st and 2nd dehydration step in the temperature range between 275 to 350°C, which is observed in the IR-spectra of the samples taken after each TG run (Fig. 6), a temperature range which has not been considered further, therefore. For the first step a loss of 3.3 wt% is expected due to dehydration. The volume fraction of $BO(OH)_2$-cage filling species is simply given by the relative mass loss fraction related to the first stage of dehydration taken as 100 %. (Note that it is a good assumption that all cages posses the same volume, irrespectively of being dehydrated or not). Assuming crystal spheres of radius, e.g. r_1 = 0.075 µm and r_2 = 0.05 µm and t = 600 s (holding time at respective temperatures) some provisional diffusion coefficients are obtained as shown in Fig. 8 with full triangles up and down, respectively. It is observed that extrapolation of eq. 1 rather closely approach D_P obtained with r_1, however, only up to about 180°C from below, i.e. up to about 30 % of dehydration. For larger dehydrations the increase of D_p drops relative to the expected diffusion coefficients. An increase of dehydration could be expected due to the small crystal size and superimposition of diffusion profiles from all sites of the crystal. However, contrary the decrease in water content and increase in $BO(OH)_2$-cage filling species obviously leads to a drop of D_p. A possible explanation could be related to a stabilization effect by $NaBO(OH)_2$-SOD formation beside an ordinary decrease in the effective gradient due to the reduction in H_2O content (break down of semi infinite medium).

We are aware that the good approach of the dashed line to D_P at lower temperature could be rather accidental. First of all the assumption of spherical crystals of unique size is certainly not justified. However, a distribution around an average value could compensate each other and D_P may, therefore, be a good approximation for $<D_P>$. An average crystal size of the order of r_1 could also be justified by peak width evaluations of XRD pattern using the Scherrer equation [29]. A more serious problem is the holding time (600 s) along with probably a too slow heating rate in the TG experiments. However, a correction of the drop in D_p with t in eq. 1 would lead to much shorter effective holding times than taken. Instead an effectively longer holding time could be more reliable taking into account the heating rate, which would lead to a larger drop in D_p.

Finally the calculated values D_p for dehydration of $NaBO(OH)_2$-SOD for the powder related data may be considered as shown in Fig. 8, too (open triangles). The IR spectra show no $B(OH)_4$-species at the temperatures considered here. However, the denoted activation energy may be rather arbitrary as long as not justified by appropriate single crystal data or at least some more data points available for the limit of a low density of BO_2-cage filling species in the $NaB(OH)_2$-SOD. Nevertheless somewhat smaller activation energy for dehydration diffusion in $NaB(OH)_2$-SOD compared to $NaB(OH)_4$-SOD could be suggested due to the larger lattice parameter and the higher probability of cage opening at the higher temperature processed.

5. Conclusion

The extrapolation of the data obtained on large single crystal by the micro Raman-technique at temperatures well in the stability field of $NaBO_2$-SOD rather closely describes the dehydration of small $NaB(OH)_4$-crystals at lower temperatures with the same activation energy. This indicates that the same diffusion mechanism occurs for dehydration of NaB(OH)4-crystals at higher temperatures and lower temperatures as long as the limit of low defect concentrations, $BO(OH)_2$-species in the $NaB(OH)_4$-crystal is justified. An opening of the sixring windows may be realized by sufficient defect formations on Na sites. This may presently suggested considering the data reported Levi and Lutze [12] for Na self diffusion for NaCl-SOD. A more direct verification for $NaB(OH)_4$-SOD seems to be interesting for future work. Whether dehydration occurs by separated jumps of OH^- and H^+ out of the cage or by initial formation of H_2O remain also open. At least the fast HD exchange indicate a high and independent ability of defect formation in the proton sublattice of $NaB(OH)_4$-SOD. Comparison with the effects observed during dehydration of hydro and basic-hydrosodalite may show that stabilisation effects of intermediate phases during dehydration well lead to deviations of formally calculated diffusion coefficients beside an ordinary decrease of the effective gradient.

Acknowledgement: Work supported by DFG (RU764/6-1)

References

[1] W. H. Baur, R. X. Fischer: *A historical note on the sodalite framework: The contribution of Frans Maurits Jaeger*. Microp. Mesopor. Mater. **116**, 1-3 (2008).
[2] R. X. Fischer, W. H. Baur: *Symmetry relationships of sodalite (SOD) – type crystal structures*. Z. Kristallogr. **224**, 185-197 (2008).
[3] C. H. Rüscher, T. M. Gesing, J. C. Buhl : *Anomalous thermal expansion behaviour of $Na_8[AlSiO_4]_6(NO_3)_2$-sodalite: P4-3n to Pm3-n phase transition by untilting and contraction of TO_4 units Z. Kristallogr*. **218**, 332-344 (2003).
[4] C. M. B. Henderson, D. Taylor: *Infrared spectra of anhydrous members of the sodalite family.* Spectrochim. Acta 33A 283-290 (1977)
[5] D. Taylor: *Cell Parameter correlations in the aluminosilicate-sodalites*. Contrib. Mineral. Petrol. **51**, 39-47 (1975).
[6] G. M. Canfield, M. Bizimis, S. E. Latturner: *Sodalite ion exchange in polyethylene oxide oligomer solvents*. J. Mater. Chem. **17**, 4530-4534 (2007).
[7] R. M. Barrer, J. D. Falconer: *Ion exchange in felspathoids as a solid state reaction*. Proc. Royal Sociiety London Series **A 236**, 227-249 (1956).
[8] J. Felsche, S. Luger: *Structural Collapse or expansion of the hydro sodalite series $Na_8[AlSiO_4]_6(OH)_2\bullet nH_2O$ and $Na_6[AlSiO_4]_6\bullet n(H_2O)$ upon dehydration*. Ber. Bunsenges. Phys. Chem. **90**, 731-736 (1986).
[9] J. Felsche, S. Luger: Phases and thermal decomposition characteristics of hydro-sodalites $Na_{6+x}[AlSiO_4]_6(OH)_x\bullet nH_2O$. Thermochimica Acta 118, 35-55 (1987).
[10] R. M. Barrer, E. A. Saxon-Napier: Dielectric properties of basic sodalite and a silver nitrate-zeolite complex. Trans. Faraday Soc. 58, 145-155 (1962).
[11] R. F. Sippel: *Sodium self diffusion in natural minerals*. Geochimica Acta **27**, 107-120 (1963).
[12] H. W. Levi, W. Lutze: *Sodium self diffusion in sodalite by heterogeneous isotopic exchange*. Phys. Stat. sol. **A 5**, K 159- K161 (1971).
[13] Y. Pan, P. Dong: *Bromine in Scapolite-group minerals and sodalite: XRF microprobe analysis, exchange experiments, and application to skarn deposits.* The Can. Mineralogist **41**, 529-540 (2003).
[14] J. C. Buhl, G. Engelhard, J. Felsche: *Synthesis, Xray diffraction and MAS NMR characteristics of tetrahydroxoborate sodalite $Na_8[AlSiO_4]_6(B(OH)_4)_2$*. Zeolites **3**, 40-44 (1989).
[15] J. C. Buhl, C. Mundrus, J. Löns, W. Hofmann: *On the enclathration of NaB(OH)4 in the b-cages of sodalite: Crystallization linetics and crystal structure*. Z. Naturforsch. **49a**, 1171-1178 (1994).
[16] J. C. Buhl, S. Luger: *The properties of salt–filled sodalites. I. Thermal decomposition reactions of hydroxoborate sodalite*. Thermochimica Acta **168**, 253-259 (1990).
[17] H. H. E. Pietsch, M. Fechtelkord, J. C. Buhl: *The formation of unusually twofold coordinated boron in a sodalite matrix*. J. Alloys Compd. **257**, 168- 174 (1997).
[18] C. H. Rüscher: *Chemical reactions and structural phase transitions of sodalites and cancrinites in temperature dependent infrared (TIR) experiments*. Microp. Mesop. Materials **86**: 58-68 (2005).
[19] J. C. Buhl, T. M. Gesing, C. H. Rüscher: *Synthesis, crystal structure and thermal stability of tetrahydroborat sodalite $Na_8[AlSiO_4]_6(BH_4)_2$*. Micropor. Mesopor. Mater. **80**, 57-63, 2005.
[20] J. C. Buhl, L. Schomborg, C. H. Rüscher: *Tetrahydroborate sodalite nanocrystals: Low temperature synthesis and thermally controlled intra cage reactions for hydrogen release of nano- and micro crystals*. Micro. Meso. Mater. **132**, 210-218 (2010).
[21] J. C. Buhl, L. Schomborg, C. H. Rüscher: *Enclosure of sodium tetrahydroborate ($NaBH_4$) in solidified aluminosilicate gels and microporous crystalline solids for fuel processing*. In Hydrogen Storage ed. By J. Liu. Intech free online edition www.intechopen.com, **Chapter 3**, 49-90 (2012).
[22] D. M. Ruthven, S. Brandani, M. Eic: In: *Adsorption and Diffusion*, ed. H. G. Karge and J. Weitcamp, Springer Berlin Heidelberg 7, 45-85 (2008).
[23] C. Chmelik, J. Kärger: *In situ study on molecular diffusion phenomena in nanoporous catalytic solids*. Chem. Soc. Rev. **39**, 4864-4884 (2010).
[24] J. Kärger, R. Valiullin: *Mass transfer in mesoporous materials: the benefit of microscopic diffusion measurement*. Chem. Soc. Rev. **42**, 4172-4197 (2013).
[25] J. Crank: *The mathematics of diffusion*. Clarendon Press Oxford, pp 23-39. (1975)
[26] A. G. Schneider, T. Bredow, L. Schomborg, C. H. Rüscher: *Structure and IR vibrational spectra of $Na_8[AlSiO4]_6(BH_4)_2$: Comparison of Theory and Experiment*. J. Phys. Chem. **A 118 (34)**, 7066-7073 (2014).
[27] R. K. McMullan, S. Ghose, N. Haga, V. Schomaker: *Sodalite $Na_4Si_3Al_3O_{12}Cl$: Structure and ionic mobility at high temperatures by neutron diffraction*. Acta Cryst. **B 52**, 616-627 (1996).
[28] A. G. Schneider, A. C. Ulpe, T. Bredow, L. Schomborg, C. H. Rüscher: *Structure, vibrational spectra and chemical shift of $Na_8[AlSiO_4]_6(B(OH)_4)_2$: Comparison of theory and experiment*. in progress
[29] A. Schulz, C. H. Rüscher, J. C. Buhl: *Synthesis and characterisation of nano- and micro-sized NaB(OH)4-sodalites*. Z. Krist.Suppl. Iss No. **31**, 91 (2011).